# Hydrodynamics of superfluid helium below 0.6 °K. III. Propagation of temperature waves*

Humphrey J. Maris
*School of Mathematics and Physics, University of East Anglia, Norwich, England*†
*Institute of Theoretical Physics, Göteborg, Sweden*
*Department of Physics, Brown University, Providence, Rhode Island*‡
(Received 4 September 1973)

The propagation of second-sound waves in superfluid helium is considered for temperatures below 0.6 °K. A dispersion relation for the waves is obtained. This relation is valid for frequencies much less than the small-angle phonon-phonon collision rate. In the low-frequency limit the usual second-sound mode with velocity $c_0/\sqrt{3}$ is found ($c_0$ is the phonon velocity). At higher frequencies the velocity of this mode increases towards $c_0$, and other modes of lower velocity appear. The nature of these waves is discussed. Finally, several experiments that might give information about the waves are considered.

## I. INTRODUCTION

The existence of second sound in superfluid helium-4 was first proposed by Tisza[1] and by Landau.[2] The first experimental observations were made by Peshkov.[3] Second sound is a collective oscillation of the gas of phonons and rotons.[4] Using the two-fluid model, Landau was able to derive the following result for the second-sound velocity $c_2$:

$$c_2^2 = \rho_s T S^2/\rho_n C\,. \tag{1}$$

$S$ and $C$ are respectively the entropy and specific heat per unit mass, and $\rho_n$ and $\rho_s$ are the densities of the normal and superfluid components. At temperatures above 1.3 °K the major contributions to the entropy, specific heat, and normal fluid density come from the roton region of the dispersion curve. In this temperature range the velocity of second sound as calculated from Eq. (1) is approximately $0.2\times10^4$ cm sec$^{-1}$. This is in good agreement with experiment.[4] At temperatures below 0.6 °K it is the phonons that dominate the thermodynamic functions. As a first approximation, the relation between the energy $\epsilon$ of a phonon and its momentum $p$ may be assumed to be linear. Thus,

$$\epsilon \approx c_0 p\,. \tag{2}$$

It is then straightforward to show that the two-fluid result for the velocity of second sound [Eq. (1)] is

$$c_2 = c_0/\sqrt{3}\,. \tag{3}$$

The velocity $c_0$ is known[5] to be $2.383\times10^4$ cm sec$^{-1}$. Hence, the velocity of second sound below 0.6 °K should be $1.38\times10^4$ cm sec$^{-1}$. Experimentally, an increase in velocity is definitely observed as the temperature is lowered below 1 °K, but different experiments seem to give different results.[6-15] The difficulty appears to be that the derivation of Eq. (1) using the two-fluid theory implicitly assumes that the mean free paths of the phonons and rotons are negligible compared to the wavelength of the second-sound wave. Thus Eq. (1), and Eq. (3), which is derived from it, must be considered as correct only for second sound of very long wavelength. When the wavelength of the second sound is comparable to the mean free path of the excitations, the second-sound velocity becomes frequency dependent and the wave is attenuated.[4] Experiments at different frequencies may then give very different results. As a practical problem, this becomes important at low temperatures because the mean free path of the excitations increases rapidly as the temperature is decreased.

In this paper the velocity of second sound is calculated as a function of frequency and temperature. We consider only the temperature range below 0.6 °K and assume that rotons may be neglected. In the next section we obtain the basic theory and formal results for the second-sound dispersion relation and the group velocity. In Sec. III we obtain numerical results for the dispersion relation. We find that at low temperatures ($T<0.4$ °K) there are other waves that can propagate through the phonon gas in addition to the usual second-sound wave. In Sec. IV we discuss various experiments that might be carried out to investigate the dispersion relations of these waves.

## II. DISPERSION RELATION FOR SECOND SOUND

Consider a superfluid containing a distribution $n_p$ of excitations. Assume that the density is uniform and that the superfluid velocity is everywhere zero.[16] The rate of change of $n_p$ with time is determined by the Boltzmann equation

$$\frac{\partial n_p}{\partial t} = \left(\frac{\partial n_p}{\partial t}\right)_{\text{coll}} - \vec{v}_p \cdot \frac{\partial n_p}{\partial \vec{X}}, \tag{4}$$

where $\vec{v}_p$ is the group velocity of an excitation, given by

$$\vec{v}_p = \frac{\partial \epsilon}{\partial \vec{p}}. \tag{5}$$

The first term on the right-hand side of Eq. (4) arises from collisions between the excitations. Suppose that $n_p$ differs only slightly from an equilibrium distribution $n_p^0$ characterized by a temperature $T$. Then, we define $\Delta n_p$ as

$$\Delta n_p \equiv n_p - n_p^0, \tag{6}$$

with

$$n_p^0 = (e^{\epsilon/k_B T} - 1)^{-1}. \tag{7}$$

The collision term may then be linearized by writing

$$\left(\frac{\partial n_p}{\partial t}\right)_{\text{coll}} = \int C(\vec{p}, \vec{p}')\Delta n_{p'}\, d\tau_{p'}. \tag{8}$$

The integral is over all of momentum space. We introduce the symmetrized collision operator[17] $\tilde{C}(\vec{p}, \vec{p}')$, defined as

$$\tilde{C}(\vec{p}, \vec{p}') \equiv C(\vec{p}, \vec{p}')[n_{p'}^0(n_{p'}^0+1)/n_p^0(n_p^0+1)]^{1/2}. \tag{9}$$

We may define eigenfunctions $\psi_i(\vec{p})$ and eigenvalues $\lambda_i$ of $\tilde{C}$ by

$$\int \tilde{C}(\vec{p}, \vec{p}')\psi_i(\vec{p}')\, d\tau_{p'} = -\lambda_i \psi_i(\vec{p}). \tag{10}$$

We now write $\Delta n_p$ as an eigenfunction expansion:

$$\Delta n_p = (n_p^0)^{1/2}(n_p^0+1)^{1/2} \sum_j A_j \psi_j(\vec{p}). \tag{11}$$

The $\{A_j\}$ are coefficients, which may depend on position and time. If we substitute Eq. (11) into Eq. (4), multiply by $\psi_i(\vec{p})$, integrate over momentum space, and use the orthogonality of the eigenfunctions, we obtain

$$\frac{\partial A_i}{\partial t} = -\lambda_i A_i - \sum_j \langle i | \vec{v}_p | j \rangle \frac{\partial A_j}{\partial \vec{X}}. \tag{12}$$

The matrix element is defined in the conventional way as

$$\int \psi_i(\vec{p}) \vec{v}_p \psi_j(\vec{p})\, d\tau_p.$$

Consider solutions of Eq. (12) in the form of plane waves propagating in the $z$ direction. Let

$$A_i = A_i^K e^{i(2\pi K z - \Omega t)}. \tag{13}$$

Then

$$\sum_j [E_{ij}(K) - \Omega \delta_{ij}] A_j^K = 0, \tag{14}$$

with

$$E_{ij}(K) = 2\pi K \langle i | v_p \cos\theta | j \rangle - i\lambda_i \delta_{ij}. \tag{15}$$

The dispersion relation for the waves is

$$\det(\vec{E} - \vec{I}\Omega) = 0, \tag{16}$$

where $\vec{I}$ is the unit matrix.

### A. Properties of the eigenfunctions

To proceed further we need to know the eigenfunctions and eigenvalues. Since $\tilde{C}(\vec{p}, \vec{p}')$ only depends on the magnitudes of $\vec{p}$ and $\vec{p}'$ and the angle between these vectors, the angular parts of the eigenfunctions must be spherical harmonics. We therefore label each eigenfunction by a radial quantum number $n \geq 1$, an "angular momentum" $l$, and a magnetic quantum number $m$. The eigenvalues need only be labeled by $n$ and $l$, since they do not depend on $m$. Eigenfunctions with the same $l$ and $m$ but different radial quantum numbers must be orthogonal. Thus, for any $lm$ combination there can be at most one eigenfunction with no radial modes.[18] If this exists, we denote it by $n = 1$. The physical meaning of the eigenvalues can be appreciated if we note that when the $\{A_i\}$ are independent of $\vec{X}$, a solution of the Boltzmann equation (4) is

$$\Delta n_p = (n_p^0)^{1/2}(n_p^0+1)^{1/2} \sum_i A_i \psi_i(\vec{p}) e^{-\lambda_i t}. \tag{17}$$

Thus, if we add to an equilibrium distribution function $n_p^0$ a perturbation proportional to $(n_p^0)^{1/2}(n_p^0+1)^{1/2}\psi_i(\vec{p})$, this perturbation decays exponentially in a time $\lambda_i^{-1}$. It follows that conserved quantities lead to eigenfunctions with zero eigenvalue. If we raise the temperature by $\Delta T$, the phonon distribution is changed by [see Eq. (7)]

$$\begin{aligned}\Delta n_p &= n_p^0(T+\Delta T) - n_p^0(T) \\ &\approx \epsilon n_p^0(n_p^0+1)\Delta T/k_B T^2.\end{aligned} \tag{18}$$

Because of energy conservation, collisions do not change this distribution. Hence, from (17) there must be an eigenfunction:

$$\psi_{100}(\vec{p}) = (\text{const.})\epsilon(n_p^0)^{1/2}(n_p^0+1)^{1/2} \quad (1S \text{ state}). \tag{19}$$

The eigenvalue $\lambda_{10}$ of this state must be zero. To make this eigenfunction normalized, we have to choose[19] the constant to be $(\beta/C\rho T)^{1/2}$, where $\beta = 1/k_B T$, $\rho$ is the density, and $C$ is the specific heat per unit mass. Conservation of momentum gives three more eigenfunctions. The eigenfunction connected with $p_z$ is

$$\psi_{110}(\vec{p}) = (\text{const.})p\cos\theta\,(n_p^0)^{1/2}(n_p^0+1)^{1/2} \quad (1P \text{ state}). \tag{20}$$

Thus

$$\lambda_{11}=0\,. \tag{21}$$

To calculate the remaining eigenfunctions we have to make specific assumptions about the form of the kernel of the collision integral. This kernel has been considered in detail in a previous paper,[20] referred to hereafter as I. The main features are as follows: The collisions between the phonons are predominantly small-angle three-phonon collisions. To calculate the collision angle, it is essential to consider the small deviations of the phonon-dispersion law from the linear approximation [Eq. (2)]. In I it was assumed that a good approximation to the dispersion relation was

$$\epsilon=c_0 p\left(1+\gamma p^2\frac{1-(p/p_A)^2}{1+(p/p_B)^2}\right). \tag{22}$$

$\gamma$, $p_A$, and $p_B$ are constants chosen so that this dispersion curve is consistent with neutron-scattering,[21] specific-heat,[22] and viscosity measurements.[23] Two sets of possible values were obtained: these values are listed in Table I, and we refer to the corresponding dispersion curves as C and D. Using the collision kernel given in I, it is straightforward to show that the eigenvalue equation (10) becomes

$$\int_0^\infty F_l(\epsilon\,,\epsilon_2)R_{nl}(\epsilon_2)\epsilon_2\,d\epsilon_2=\lambda_{nl}R_{nl}(\epsilon)\epsilon\,, \tag{23}$$

where

$$\begin{aligned}F_l(\epsilon,\epsilon_2)=\Gamma(\epsilon)\delta(\epsilon-\epsilon_2)P_l(0)&\\ -B\epsilon\epsilon_2(\epsilon-\epsilon_2)^2 f(|\epsilon-\epsilon_2|)P_l(\theta')&\\ +B\epsilon\epsilon_2(\epsilon+\epsilon_2)^2 f(\epsilon+\epsilon_2)P_l(\theta'')\,,&\end{aligned} \tag{24}$$

$$\Gamma(\epsilon)=\tfrac{1}{2}B\int_0^\epsilon \epsilon_3^2(\epsilon-\epsilon_3)^2[n^0(\epsilon_3)+n^0(\epsilon-\epsilon_3)+1]\,d\epsilon_3 +B\int_0^\infty \epsilon_3^2(\epsilon+\epsilon_3)^2[n^0(\epsilon_3)-n^0(\epsilon+\epsilon_3)]\,d\epsilon_3\,, \tag{25}$$

with

$$B=(u_0+1)^2/(4\pi\rho\hbar^4 c_0^5)\,, \tag{26}$$

$$n^0(\epsilon)=(e^{\epsilon/k_BT}-1)^{-1}\,, \tag{27}$$

TABLE I. Parameters defining the dispersion curves C and D.

| | $\gamma$ ($10^{37}$ g$^{-2}$ cm$^{-2}$ sec$^2$) | $p_A/\hbar$ (Å$^{-1}$) | $p_B/\hbar$ (Å$^{-1}$) |
|---|---|---|---|
| C | 8 | 0.5385 | 0.3727 |
| D | 10 | 0.5418 | 0.3322 |

$$f(\epsilon)=n^0(\epsilon)^{1/2}[n^0(\epsilon)+1]^{1/2}\,. \tag{28}$$

$u_0$ is the Grüneisen constant defined by

$$u_0\equiv\frac{\rho}{c_0}\frac{\partial c_0}{\partial\rho}\,.$$

Measurements by Abraham *et al.*[24] give $u_0=2.84$. The angles $\theta'$ and $\theta''$ are most conveniently defined by regarding $p$ as a function of $\epsilon$. Then,

$$\cos\theta'=\frac{p^2(\epsilon)+p^2(\epsilon_2)-p^2(|\epsilon-\epsilon_2|)}{2p(\epsilon)p(\epsilon_2)}\,, \tag{29}$$

$$\cos\theta''=\frac{p^2(\epsilon+\epsilon_2)-p^2(\epsilon)-p^2(\epsilon_2)}{2p(\epsilon)p(\epsilon_2)}\,. \tag{30}$$

Although we have explicitly indicated the limits of integration in Eqs. (23) and (25), it is to be understood that the ranges are still limited by the requirements that $\theta'$ and $\theta''$ be real.[25] $P_l(\theta)$ is the $l$th Legendre polynomial. The eigenfunction $\psi_{nlm}(\vec{p})$ is connected to the function $R_{nl}(\epsilon)$ by

$$\psi_{nlm}(\vec{p})=R_{nl}(\epsilon)Y_{lm}(\theta,\phi)\,, \tag{31}$$

where $Y_{lm}(\theta\phi)$ is a spherical harmonic, and the direction of $\vec{p}$ is defined by the angles $\theta$ and $\phi$. There are a number of approximations in these results: these are discussed in detail in I.

We have been unable to solve Eq. (23) analytically and have therefore had to use a numerical method. The technique is simply to replace the integral on the left-hand side by a sum over a finite set of points. This reduces Eq. (23) to a matrix eigenvalue problem. The number of eigenfunctions and eigenvalues found is equal to $j_m$, the number of points summed over. Consider first the solutions for $S$ states ($l=0$). If we use a set of points $j\Delta\epsilon$, where $j=1,2,\ldots,j_m$, we find the 1$S$-state eigenfunction [Eq. (19)] together with

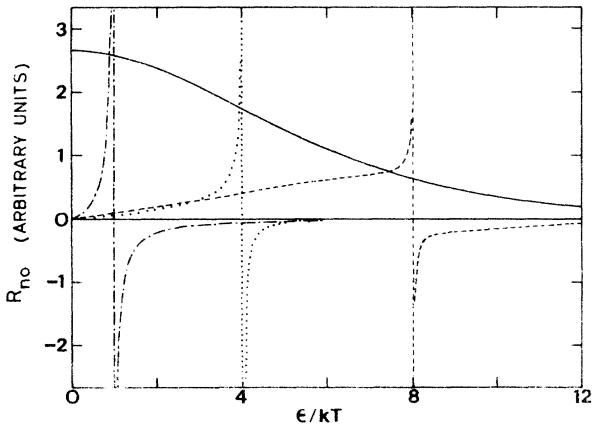


FIG. 1. Radial part $R_{n0}(\epsilon)$ of the $S$-state eigenfunctions at 0.25 °K. The 1$S$-state eigenfunction is denoted by the solid line. The remaining curves are three typical eigenfunctions from the continuous spectrum.

$j_m - 1$ eigenfunctions with finite eigenvalues. Doubling the number of points and simultaneously halving $\Delta\epsilon$ has the following results. The $1S$ state is still found. The $j_m - 1$ eigenfunctions found previously with finite eigenvalues have their eigenvalues shifted slightly. New eigenvalues appear between each of the old eigenvalues and one new eigenvalue is added above the highest eigenvalue found previously. These features imply that the eigenvalue spectrum is continuous starting at zero. This is in agreement with a result obtained by Jäckle.[26] The radial parts of some of the eigenfunctions for $T = 0.25\,^{\circ}\mathrm{K}$ are shown in Fig. 1. The $n \neq 1$ eigenfunctions all have a singularity of the form

$$A\delta(\epsilon - \epsilon_c) + B/(\epsilon - \epsilon_c)_P , \tag{32}$$

where $A$ and $B$ are constants and $P$ denotes the principal part. There may also be weaker singularities at the same point; we have not made a detailed study. The critical energy $\epsilon_c$ is related to the eigenvalue $\lambda$ by[27]

$$\lambda = \Gamma(\epsilon_c) . \tag{33}$$

The eigenfunctions and eigenvalues for $S$ states change with temperature in a simple way. Suppose that at temperature $T$ there is an eigenfunction $\psi_T(\vec{p})$ with eigenvalue $\lambda_T$. Then from Eqs. (23)–(25), it is easy to show that at temperature $T'$ there is an eigenfunction[28]

$$\psi_{T'}(\vec{p}) = \psi_T(\vec{p}T/T') . \tag{34}$$

The associated eigenvalue is

$$\lambda_{T'} = \lambda_T(T'/T)^5 . \tag{35}$$

The $l$ dependence of the eigenvalues is shown in Fig. 2. These results are for $T = 0.25\,^{\circ}\mathrm{K}$ using $j_m = 10$ and $\Delta\epsilon = 2k_BT$. The eigenvalues of the $n \neq 1$ eigenfunctions are nearly independent of $l$ and are nearly independent of which phonon-dispersion curve is assumed (C or D). The eigenvalues of the $n = 1$ states, on the other hand, increase rapidly with increasing $l$ and are significantly different for the two phonon-dispersion curves. These features arise because most collisions between phonons are small-angle collisions. Suppose an equilibrium distribution of phonons is perturbed by adding a distribution with angular dependence $P_l(\theta)$ and a radial dependence similar to that of a $1S$ or $1P$ state. To bring the system back to equilibrium, the small-angle collisions must transport the excess phonons from regions of momentum space where $P_l(\theta)$ is positive to regions where $P_l(\theta)$ is negative. This takes a long time and therefore $\lambda_{1l}$, which is the reciprocal of this time, is small. The time taken, however, does decrease rapidly with increasing $l$, since the maxima and minina of $P_l(\theta)$ come closer together. Thus, $\lambda_{1l}$ increases rapidly with $l$. The time also involves the angle of the typical collision and this is different for the two forms of the dispersion curve. On the other hand, a perturbation having $S$ symmetry and a radial mode is rapidly destroyed by small-angle collision. Thus, in general, $\lambda_{nS}$ for $n \neq 1$ is large in the sense that

$$\lambda_{nS} \gg \lambda_{1l} . \tag{36}$$

This statement has to be qualified in two regards. First, it is only true provided $l$ is not too large. The typical collision angle in the small-angle collisions is roughly $10^{\circ}$. For $l \gtrsim 15$, $P_l(\theta)$ varies considerably over a $10^{\circ}$ range, and thus only one small-angle collision is required to destroy a $1l$ state. In the second place, Eq. (36) cannot be true for all $S$ states, since the eigenvalue spectrum of these forms a continuum starting at zero. However, as can be seen from Fig. 1, the states with very small eigenvalues have eigenfunctions which are appreciable only for very small ener-

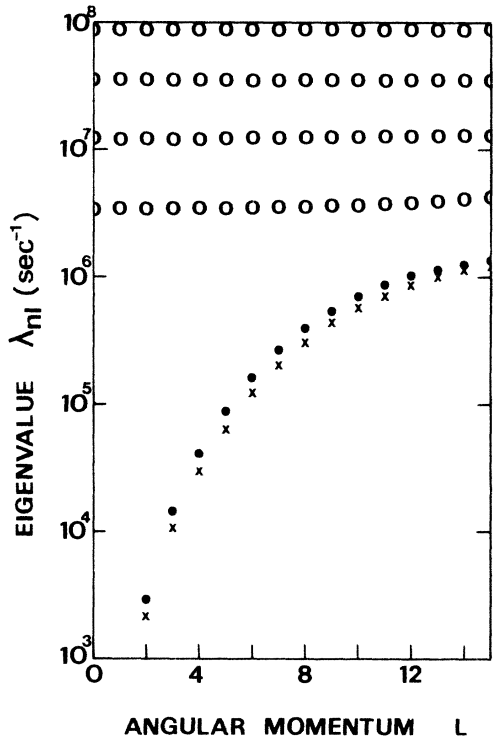


FIG. 2. Eigenvalues $\lambda_{nl}$ of the symmetrized collision operator $\tilde{C}$ as a function of the angular momentum $l$. The temperature is $0.25\,^{\circ}\mathrm{K}$. × and ● denote eigenvalues of $n = 1$ states obtained using dispersion curves C and D, respectively. The higher eigenvalues are nearly independent of whether C or D is used and are denoted by ○. Only the five lower eigenvalues are shown for each value of $l$.

gies, i.e., for $\epsilon \ll k_B T$. Subject to the same sort of qualifications, it is also true that, for $n \neq 1$,

$$\lambda_{nl} \gg \lambda_{11} . \tag{37}$$

Finally, we note that, for $n \neq 1$, $\lambda_{nS}$ is of the order of $\tau_{\parallel}^{-1}$, where $\tau_{\parallel}$ is the small-angle-collision time. The effective large-angle-collision time $\tau_{\perp}$ may be sensibly defined as

$$\tau_{\perp} = \lambda_{12}^{-1} = \lambda_{1D}^{-1} . \tag{38}$$

### B. Low-frequency approximation

Consider the propagation of a wave with frequency $\Omega$ such that

$$\Omega \tau_{\parallel} \ll 1 . \tag{39}$$

For such a wave there will be a large number of small-angle collisions in one period. Thus, one expects that for a given direction in momentum space the phonon-distribution function will be approximately described by a "temperature" and will vary smoothly with the magnitude of $\vec{p}$. It follows that in Eq. (11) the expansion coefficients $A_l$ will be very small except for the $n = 1$ states. If we restrict attention to $n = 1$ states, the elements of the matrix $\vec{\vec{E}}$ appearing in the dispersion relation (16) may be written

$$E_{lm,l'm'}(K) = 2\pi K \langle 1lm \,|\, v_p \cos\theta \,|\, 1l'm' \rangle - i\lambda_{1l}\delta_{ll'}\delta_{mm'} . \tag{40}$$

The matrix element of $\cos\theta$ vanishes unless $|m| = |m'|$. Hence, the matrix $\vec{\vec{E}}$ may be put into block diagonal form in which the blocks are characterized by definite values of $|m|$. It follows that any wave propagating through the phonon gas will be characterized by a definite number $\mu$, in the sense that the distribution function will be a linear combination of eigenfunctions with magnetic quantum numbers $\pm\mu$. Only waves with $\mu = 0$ have a nonzero value of the coefficient $A_{100}(\equiv A_{1S})$. $A_{100}$ is a measure of the fluctuation in the energy density of the phonon gas. Thus, waves with $\mu = 0$ are the easiest to detect experimentally and we will therefore concentrate on them.[29] In this case we may drop the subscripts $m$ and $m'$ and write[30]

$$\det(\vec{\vec{E}} - \vec{\vec{I}}\Omega) = 0 = \begin{vmatrix} -\Omega & 2\pi K c_0 G_1 & & \\ 2\pi K c_0 G_1 & -\Omega & 2\pi K c_0 G_2 & \\ & 2\pi K c_0 G_2 & -\Omega - i\lambda_{12} & 2\pi K c_0 G_3 \\ & & \ddots & \ddots \end{vmatrix} \tag{41}$$

where

$$G_l \equiv \langle 1\, l\, -1\, 0 \,|\, v_p \cos\theta / c_0 \,|\, 1 l 0 \rangle . \tag{42}$$

Note that $\lambda_{10}$ and $\lambda_{11}$ are zero. For any choice of the wave number $K$ we will find a number of solutions for $\Omega$ which we label by an index $\zeta$. The solution $\Omega_K^{\zeta}$ will have definite values of the coefficients $A_{nlm}$ associated with it, these satisfying Eq. (14). We denote these by $A_l^{K\zeta}$, dropping the $n$ and $m$ subscripts which from now on will always have the values 1 and 0, respectively. Using Eqs. (11), (13), and (31), we find that the phonon-distribution function associated with the wave $K\zeta$ is

$$\Delta n_p = (2\pi)^{-1/2}(n_p^0)^{1/2}(n_p^0+1)^{1/2} e^{i(2\pi K z - \Omega_K^{\zeta} t)} \times \sum_l A_l^{K\zeta} P_l(\theta) R_l(\epsilon) . \tag{43}$$

We have dropped the $n$ subscript on $R_{nl}(\epsilon)$. Since $E_{ll'}$ is a symmetric matrix, we may choose the $A_l^{K\zeta}$ so that

$$\sum_l A_l^{K\zeta} A_l^{K\zeta'} = \delta_{\zeta\zeta'} . \tag{44}$$

To calculate the group velocity of the wave $K$, we may use perturbation theory. Consider a small variation $\Delta K$ in $K$. Let

$$\Delta E_{ll'} \equiv E_{ll'}(K + \Delta K) - E_{ll'}(K) = 2\pi \Delta K (G_l \delta_{l+1,l'} + G_{l'} \delta_{l,l'+1}) . \tag{45}$$

Then, to first order in $\Delta K$,

$$\Omega_{K+\Delta K}^{\zeta} - \Omega_K^{\zeta} = \sum_{ll'} A_l^{K\zeta} \Delta E_{ll'} A_{l'}^{K,\zeta} = 4\pi \Delta K c_0 \sum_l A_l^{K\zeta} G_l A_{l+1}^{K\zeta} . \tag{46}$$

Thus, the group velocity is

$$v_{\text{group}\,K}^{\zeta} = (\Omega_{K+\Delta K}^{\zeta} - \Omega_K^{\zeta})/2\pi\Delta K = 2c_0 \sum_l A_l^{K\zeta} G_l A_{l+1}^{K\zeta} . \tag{47}$$

## III. NUMERICAL RESULTS

### A. Small-angle collision rate

Consider first the small-angle-scattering time $\tau_{\parallel}$. We need to know this to estimate the range of frequencies for which the "low-frequency ap-

proximation" is valid [see Eq. (39)]. The collision rate for a phonon of energy $\epsilon$ is $\Gamma(\epsilon)$, as given by Eq. (25). The lifetime $\tau_{\|}$ is thus

$$\tau_{\|} = 1/\Gamma(\epsilon) . \tag{48}$$

We also define a mean free path $\Lambda_{\|}$ by

$$\Lambda_{\|} = c_0 \tau_{\|} . \tag{49}$$

The temperature and energy dependence of $\tau_{\|}$ and $\Lambda_{\|}$ are shown in Fig. 3. To apply Eq. (39), let us define $\bar{\tau}_{\|}$ as the lifetime of a "typical" thermal phonon. We take the energy of the typical phonon to be $3k_B T$. Then,

$$\bar{\tau}_{\|} = 2.62 \times 10^{-10} T^{-5} \text{ sec} . \tag{50}$$

Thus, the frequency condition (39) becomes

$$\nu \ll 608 T^5 . \tag{51}$$

where $\nu$ is the frequency in MHz.

### B. Dispersion relation

To find the frequency as a function of wave number, we must solve the determinantal equation (41). To do this, we have to truncate the infinite determinant at some finite value of $l$, which we call $l_{\max}$. This gives $(l_{\max}+1)$ solutions for $\Omega_K^{\zeta}$ and the coefficients $A_l^{K\zeta}$. Of these solutions, those with lower frequency have coefficients $A_l^{K\zeta}$, which decrease rapidly as $l$ increases beyond some critical value $l_c$. If $l_{\max}$ is sufficiently greater than $l_c$, these solutions are found to be independent of $l_{\max}$. Values of $l_{\max}$ up to 16 were used. For any given choice of $l_{\max}$, there are always some high-frequency solutions for which even $A_{l_{\max}}^{K\zeta}$ is of the same order of magnitude as $A_0^{K\zeta}$. These solutions change radically even if $l_{\max}$ is increased by 1 and therefore were discarded.

Using this method, we have investigated the dispersion relation ($\Omega$ vs $K$) for a number of temperatures between 0.15 and 0.6 °K. In Fig. 4 we show results obtained for the complex phase velocity $v$ defined as

$$v = \Omega/2\pi K . \tag{52}$$

These results are for $T = 0.25$ °K and assume dispersion curve C (Table I). From Eq. (41) it is clear that when $K = 0$, solutions are

$$\Omega = -i\lambda_{1l} . \tag{53}$$

Since $\lambda_{10}$ and $\lambda_{11}$ are both zero, there are two solutions of zero frequency. When $K$ is finite, these two solutions split. For very small $K$ these solutions become

$$\Omega = \pm 2\pi K c_0 G_1 . \tag{54}$$

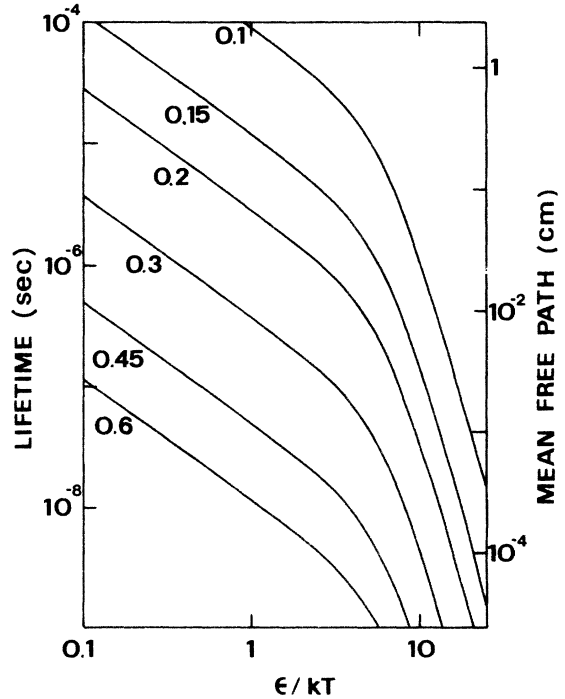


FIG. 3. Small-angle collision time $\tau_{\|}$ and mean free path $\Lambda_{\|}$ as a function of reduced phonon energy $\epsilon/k_B T$. The different curves are labeled by the temperature in °K.

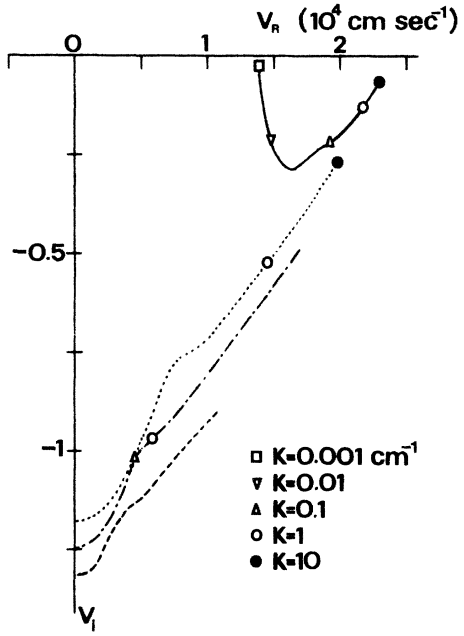


FIG. 4. Dispersion relation at 0.25 °K plotted in the complex velocity plane. Ordinary (first) second sound (———), second second sound (·····), third second sound (— — —), fourth second sound (----).

If the dispersion of the phonons is small, the group velocity $v_p$ is approximately equal to $c_0$. The matrix element $G_1$ [Eq. (42)] is then determined completely by the angular factors and equals $1/\sqrt{3}$. The velocity of these solutions is thus

$$v = \pm c_0/\sqrt{3}\,. \tag{55}$$

This is the velocity usually associated with second sound [see Eq. (3)]. We therefore call this branch of the dispersion relation first second sound. For larger $K$, the velocity of this branch increases and becomes complex. The other roots remain on the imaginary axis initially, but eventually two roots meet and split into a pair of the form

$$\pm\Omega_R + i\Omega_I\,.$$

We call these branches of the dispersion relation second second sound, third second sound, etc., according to the sequence in which they leave the imaginary axis for increasing $K$.

### C. Phonon distribution associated with the waves

Knowing the expansion coefficients, we may work out the phonon distribution function associated with the waves using Eq. (43). To express the results in a simple form, we consider $\Delta T(\theta)$, a direction-dependent "temperature change" of the phonon gas. We define this as

$$\Delta T(\theta) = \frac{k_B T^2 \int_0^\infty \Delta n_p(\theta)\epsilon p^2\,dp}{\int_0^\infty \epsilon^2 n_p^0(n_p^0+1)p^2\,dp}\,. \tag{56}$$

This definition makes $\Delta T(\theta)$ proportional to the energy density of phonons travelling in direction $\theta$. It also has the property that if the distribution of phonons is actually an equilibrium distribution characterized by a temperature $T+\Delta T$ [see Eq. (18)], then $\Delta T(\theta)$ is equal to $\Delta T$. We can simplify Eq. (56) by relating the integral in the denominator to the specific heat $C$. This gives

$$\Delta T(\theta) = \frac{4\pi}{\rho C h^3}\int_0^\infty \Delta n_p(\theta)\epsilon p^2\,dp\,. \tag{57}$$

The value of $\Delta T(\theta)$ associated with the wave $K\zeta$ may now be calculated using $\Delta n_p$ as given by Eq. (43). The result is

$$\Delta T(\theta) = h^{-3}(2T/C\rho\beta)^{1/2}\sum_l A_l^{K\zeta}P_l(\theta) \times \int_0^\infty R_l(\epsilon)R_0(\epsilon)p^2\,dp e^{i(2\pi Kz - \Omega_K^\zeta t)}\,. \tag{58}$$

Since the dispersion of the phonons is small, we may make the approximation

$$\int_0^\infty R_l(\epsilon)R_0(\epsilon)p^2\,dp \approx c_0^{-3}\int_0^\infty R_l(\epsilon)R_0(\epsilon)\epsilon^2\,d\epsilon\,. \tag{59}$$

If $l=0$, the integral over $\epsilon$ gives 1 because the radial parts of the eigenfunctions are normalized. For $l\neq 0$ we approximate the integral by 1. Provided $l<10$, this gives an error less than about 15% at all temperatures. For $l>10$ the error in approximating the integral by 1 becomes progressively larger, but the coefficients $A_l^{K\zeta}$ are very small for these values of $l$. We obtain now for the temperature in direction $\theta$

$$T+\Delta T(\theta) = (hc_0)^{-3}(2T/C\rho\beta)^{1/2} \times \sum_l A_l^{K\zeta}P_l(\theta)e^{i(2\pi Kz - \Omega_K^\zeta t)}\,. \tag{60}$$

In Fig. 5 we show some typical results for $T+\Delta T(\theta)$ as a function of the reduced phase $\phi_{\rm red}$ defined by

$$\phi_{\rm red} = \Omega_K^\zeta t - 2\pi Kz\,. \tag{61}$$

The results are shown as a polar plot as a function of $\theta$. The amplitude of the wave has been arbitrarily chosen to obtain a convenient polar plot [i.e., the $A_l^{K\zeta}$ are not normalized according to Eq. (44)]. The results are calculated for $T=0.25$ °K and assume dispersion curve C. Figures 5(a) and 5(b) show results for first second sound with wave numbers 0.3 and 10 cm$^{-1}$. For a very-low-

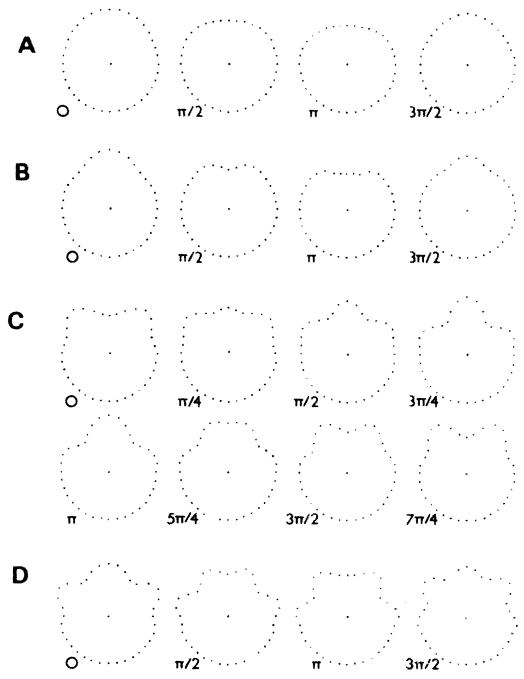


FIG. 5. Polar plots of the direction-dependent temperature $T+\Delta T(\theta)$ for first second sound $K=0.3$ cm$^{-1}$ (a), and $K=10$ cm$^{-1}$ (b), second second sound $K=3$ cm$^{-1}$ (c), and third second sound $K=3$ cm$^{-1}$ (d). These results are for $T=0.25$ °K.

frequency second-sound wave, the angular dependence of $\Delta T(\theta)$ is

$$(\text{const.})(\cos\theta + 1/\sqrt{3}) .$$

It can be seen from Figs. 5(a) and 5(b) that, as the wave number increases, $\Delta T(\theta)$ varies more rapidly with $\theta$ and becomes concentrated around $\theta = 0$. Figure 5(c) shows results for the second second-sound wave. The distribution function evolves with time in an interesting way. A bulge grows at $\theta = 0$ (phase $\pi/4$ to $3\pi/4$), which then converts into a ring (phase $\pi$ to $5\pi/4$). The ring expands to larger values of $\theta$ (phase $3\pi/2$ to $2\pi + \pi/4$) and eventually fades away while a new bulge is being formed at $\theta = 0$ (phase $2\pi + \pi/4$ to $2\pi + 3\pi/4$). A similar cycle is followed by the third second-sound wave [Fig. 5(d)] but the pattern is more complicated. The coefficients $A_l^{K\xi}$ have been chosen so that $A_0^{K\xi}$ is real. To see what this means we note that the average value of $\Delta T(\theta)$ is

$$\langle \Delta T \rangle = \tfrac{1}{2} \int_{-1}^{1} \Delta T(\theta)\, d(\cos\theta)$$
$$= (\hbar c_0)^{-3} (T/C\rho\beta)^{1/2} A_0^{K\xi} e^{i(2\pi K z - \Omega_K^{\xi} t)} . \qquad (62)$$

Thus, the effect of choosing $A_0^{K\xi}$ as real is to make $\langle \Delta T \rangle$ a maximum at phase zero.

### D. Note on allowed range of temperature

In the Introduction we mentioned that below 0.6 °K the phonons dominate the thermodynamic functions. We used this fact to justify neglecting the rotons. This argument needs some qualification. At 0.6 °K the rotons contribute only about 2% of the total entropy of the liquid. However, since the roton entropy varies rapidly with temperature, the importance of rotons is much greater as far as the specific heat is concerned. At 0.6 °K $C_{\text{roton}}$ is approximately 10% of the total specific heat. Because the momentum of the rotons is large in relation to their energy, there is also a large roton contribution to the normal fluid density (~60% at 0.6 °K).

The effect of the rotons on the propagation of second sound is not entirely clear. In the limit of very low frequencies where the two-fluid theory applies, we may calculate the second-sound velocity using Eq. (1). At 0.6 °K including the rotons in the thermodynamic functions gives $c_2 = 0.83 \times 10^4$ cm sec$^{-1}$. This is a large correction, since, if only the phonons are considered, $c_2 = 1.38 \times 10^4$ cm sec$^{-1}$. The correction does decrease rapidly at lower temperatures, however, and at 0.45 °K is only 2%.

It might also appear possible that collisions between phonons and rotons could significantly contribute to the over-all phonon-scattering rate. Landau and Khalatnikov[31] have calculated the total cross section for scattering of an $xk_BT$-energy phonon by a roton. Their result is

$$\sigma \approx 7 \times 10^{-19} (xT)^4 \text{ cm}^2 . \qquad (63)$$

At 0.6 °K the number of rotons per cm$^3$ is $2 \times 10^6$. Hence, the mean free path for a $3k_BT$ phonon is 7 cm, and the phonon mean free time due to this scattering process is $3 \times 10^{-4}$ sec. Thus, this process is unimportant compared to the three-phonon scattering mechanism. In fact, it is so weak that for second sound in the frequency range of experimental interest the rotons may take no part in the wave motion. If the phonon gas has a drift velocity $v$ relative to the roton gas, it will take of the order of $3 \times 10^{-4}$ sec for the two gases to reach the same velocity. Thus, if the frequency of the second sound is 10 kHz or greater, it appears that the rotons have very little effect on the propagation of the phonons. This is consistent with the very recent experiments of Dynes *et al.*[14] In a heat-pulse experiment at 0.55 °K they observed two separate pulses with different veloc-

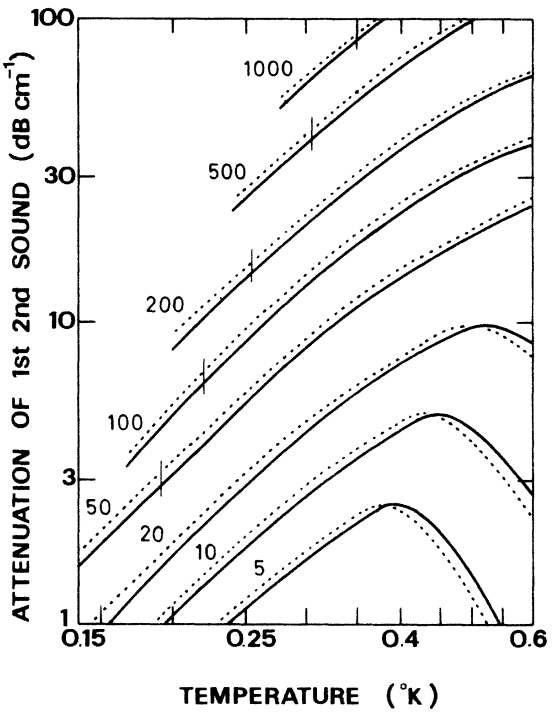


FIG. 6. Attenuation of first second sound as a function of temperature. The curves are labeled by the frequency in kHz. Results obtained using dispersion curves C and D are shown as (———) and (---), respectively. The vertical bars denote the temperatures at which $\Omega\tau_{\parallel} = 0.3$, and the curves are plotted up to $\Omega\tau_{\parallel} = 1$.

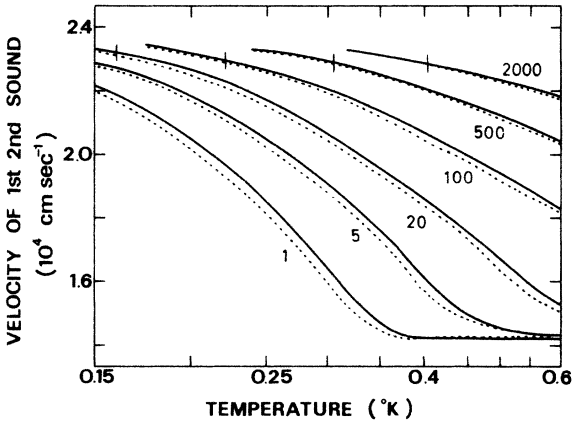


FIG. 7. Velocity of first second sound as a function of temperature. The notation is as in Fig. 6.

ities, these arising from separate collective excitations in the phonon and roton gases.

## IV. ANALYSIS OF POSSIBLE EXPERIMENTS

In this section we will consider in detail a number of experiments that might be performed to check the theory.

### A. Response to a sine wave

A simple method for investigating the characteristics of temperature waves in helium is to use a plane heater whose temperature varies sinusoidally with time. The phase and magnitude of the temperature oscillations in the liquid can then be measured as a function of $z$, the distance from the plane. For a given real value of the frequency $\Omega$, it is possible to solve the dispersion relation (41) for the complex wave number $K$. The waves with $\mathrm{Im}(K)>0$ can then be used to form a suitable linear combination to satisfy the boundary conditions at the surface of the heater. The temperature $\langle \Delta T \rangle$ at a distance $z$ into the liquid is then given by an expression of the form

$$\langle \Delta T \rangle = \sum_{\zeta} a_{\zeta} e^{i(2\pi K_{\zeta} z - \Omega t)}, \tag{64}$$

where $K_{\zeta}$ is the complex wave number of the $\zeta$th wave, and $a_{\zeta}$ are coefficients determined by the boundary conditions. The dependence of $\langle \Delta T \rangle$ on $z$ is thus very complicated for small $z$, but for large $z$ only those waves with small attenuation will make an appreciable contribution. The two least-attenuated waves are first and second second sound. We define the attenuation $\alpha_{\zeta}$ and phase velocity $v_{\zeta}$ by

$$\alpha_{\zeta} = -\mathrm{Im}(K_{\zeta})/2\pi, \tag{65}$$

$$v_{\zeta} = \Omega/2\pi\,\mathrm{Re}(K_{\zeta}). \tag{66}$$

The frequency and temperature dependence of $\alpha_{\zeta}$ and $v_{\zeta}$ for first and second second sound are shown in Figs. 6–9. For first second sound, results are shown down to a temperature at which $\Omega\tau_{\parallel}=1$. The second second-sound results are calculated only down to the temperature at which $\Omega\tau_{\parallel}=0.3$, since at lower temperatures the approximation of taking only the first 16 angular momentum states becomes inadequate.

It can be seen that the attenuation of the first second-sound wave is considerably less that of

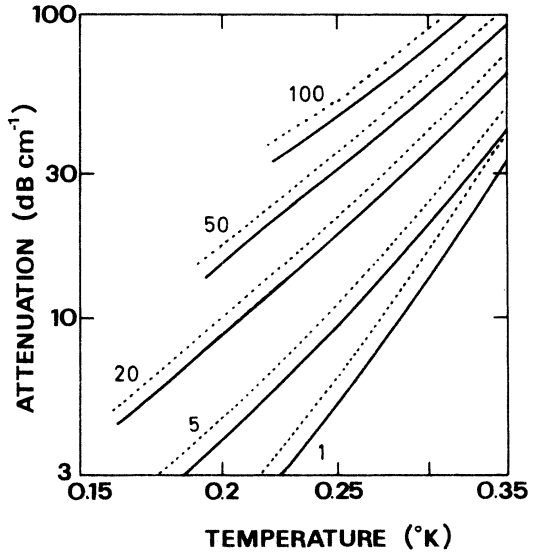


FIG. 8. Attenuation of second second sound as a function of temperature. The notation is the same as in Fig. 6, except that results are shown only up to $\Omega\tau_{\parallel}=0.3$.

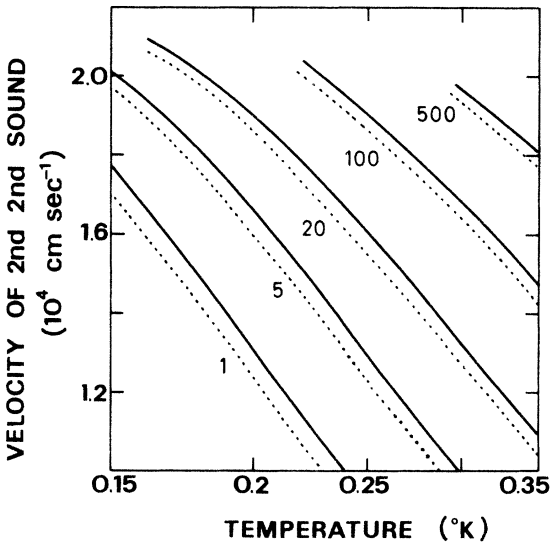


FIG. 9. Velocity of second second sound as a function of temperature. The notation is as in Fig. 8.

second second sound. Thus for large distances from the heater, a single-exponential decay should be observed. For smaller distances where the second second-sound wave is not completely attenuated, interference between the two waves should occur. To get an idea of how large an effect this might be, we have to estimate the coefficients $a_1$ and $a_2$ for the two waves. This requires some assumptions about the boundary condition at the surface of the heater. We have investigated two simple models. If the surface of the heater is undamaged and very smooth, the radiated phonons should all have momenta within a few degrees of the normal to the surface. This happens because of refraction at the interface.[32] We therefore consider a model (the refraction model) in which $\Delta T(\theta)$ at $z=0$ is

$$\Delta T(\theta) = 4\delta(1-\cos\theta)e^{-i\Omega t}. \tag{67}$$

We have arranged this so that $\langle \Delta T \rangle$, the average of $\Delta T(\theta)$ over all angles, has unit magnitude. We now calculate the $a_\zeta$ coefficients to match this boundary condition. This gives the interesting result that, in general, $a_1$ and $a_2$ are of about equal magnitude but have opposite signs. For a 50 kHz wave at 0.25 °K, for example, we find

$$\begin{aligned} a_1 &= 2.6 - 0.1i, \\ a_2 &= -2.3 + 0.1i. \end{aligned} \tag{68}$$

The reason for this phase difference can be understood from Fig. 5. With the boundary condition (67) the phases of the various waves must be such that they each give as large a contribution as possible at $\theta=0$. To achieve this we have to add a phase shift of approximately $\pi$ to the second second-sound wave. The angularly-averaged temperature $\langle \Delta T \rangle$ associated with this wave is then of opposite phase to $\langle \Delta T \rangle$ for the first second-sound wave.

The other model we have considered is intended to represent the radiation of phonons from a rough or damaged surface. We assume that at $z=0$:

$$\begin{aligned} \Delta T(\theta) &= 2e^{-i\Omega t}, \quad 0 \le \theta \le \pi/2, \\ &= 0, \qquad \pi/2 < \theta. \end{aligned} \tag{69}$$

We call this the isotropic model. In this case $a_1$ and $a_2$ are generally of the same sign. A 50-kHz wave at 0.25 °K has, for example,

$$\begin{aligned} a_1 &= 0.9 + 0.2i, \\ a_2 &= 1.0 + 0.3i. \end{aligned} \tag{70}$$

The propagation of sine waves has been studied

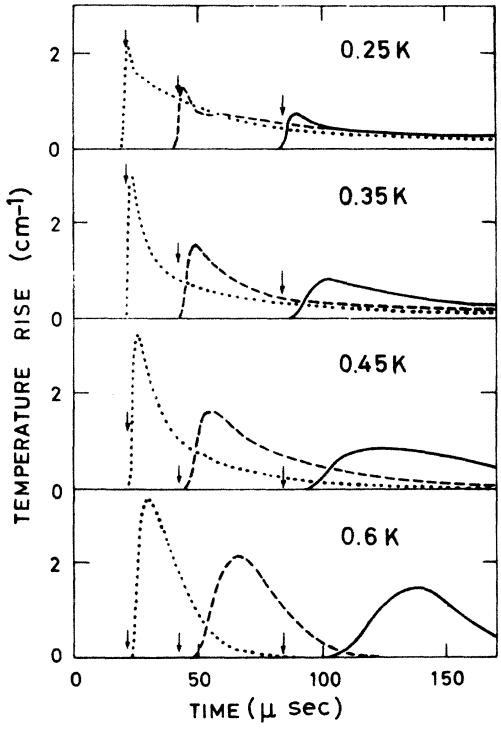


FIG. 10. Propagation of heat pulses assuming the isotropic boundary condition. The detector distances are 0.5 cm (·····), 1 cm(----) and 2 cm (———). The arrows show the arrival time for a pulse travelling with velocity $c_0$.

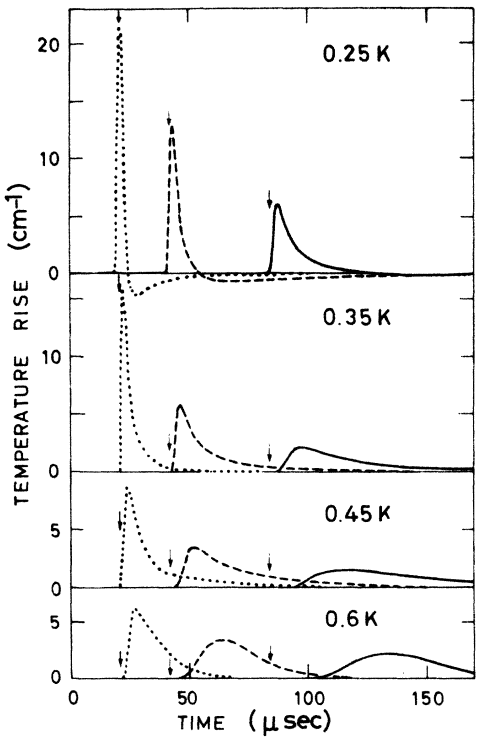


FIG. 11. Propagation of heat pulses assuming the refraction boundary condition. The notation is as in Fig. 10.

by Osborne.[15] Unfortunately, the experiments were carried out at very low frequencies between 60 Hz and 2 kHz. This corresponds to wavelengths between 10 and 300 cm. The waves were propagated along tubes 2 cm in diameter and between 0.38 and 12.35 cm long. It does not seem possible to compare the plane-wave theory we have developed here with these data. The main difficulty is that the wavelength $\lambda$ is large compared to the tube diameter $d$. To obtain the "free-space" velocity and attenuation from the experimental results requires very complicated and uncertain corrections.

One final point should be made about sine-wave experiments. The theory we have developed does not apply at distances from the heater which are comparable to the phonon mean free path $\Lambda_{\|}$ (Fig. 3). In this range of distances there will be a substantial number of phonons that travel ballistically from the heater to the detector. For a path length of 1 cm this places a low-temperature limit on the theory of about 0.15 °K.

### B. Propagation of pulses

Consider again a plane heater with normal in the $z$ direction. In a typical pulse experiment the temperature of the heater is raised for some time $\tau$ (typically between 1 and 50 $\mu$sec). Phonons are radiated and the temperature of a detector at a distance $d$ is measured as a function of time. To approximate what happens in this type of experiment, we assume that at time zero the temperature distribution in the liquid is

$$\Delta T(\theta, z) = f(\theta)\delta(z) . \tag{71}$$

We will let $f(\theta)$ have the angular dependence of the refraction or isotropic models of Sec. IV A. It is then a problem in Fourier analysis to find a linear combination of plane waves satisfying the initial condition (71). The angularly-averaged temperature $\langle \Delta T \rangle$ at later times may then be calculated in the form

$$\langle \Delta T(z, t) \rangle = \sum_{K\zeta} b_{K\zeta} e^{i(2\pi K z - \Omega_K^{\zeta} t)} , \tag{72}$$

where $b_{K\zeta}$ are coefficients determined by the initial condition.[33]

We have made calculations of pulse propagation for a variety of temperatures and propagation distances. Some typical results are shown in Fig. 10 for the isotropic model and in Fig. 11 for the refraction model.[34] Results for the velocity of the front (20% of peak height) and peak of the pulse are shown in Table II.

In these calculations the magnitude of $f(\theta)$ has been chosen so that

$$\bar{f} = \tfrac{1}{2} \int_{-1}^{1} f(\theta)\, d(\cos\theta) = 1 .$$

Since $\Delta T(\theta, z)$ is a $\delta$ function at the origin at time zero, these calculations correspond physically to the application of a very short pulse at the origin at time zero. To approximate what happens for a finite-length pulse of arbitrary shape, we could, in principle, simply add up the contributions from a number of sources of the form (71), but retarded suitably in time.

It is necessary to treat carefully the infinite Fourier spectrum of the $\delta$ function in Eq. (71). For large $K$ the imaginary part $\Omega_I$ of the frequency becomes large and negative for all of the waves. Thus, to calculate $\Delta T(\theta, z)$ at, or later than, some time $t_0$, it is sufficient to consider only those $K$ values up to some maximum $K_m$ such that $|\Omega_I| t_0 \gg 1$ for all waves with this wave number. In the present problem we are concerned with times greater than the time at which the front of the pulse arrives at the detector. Thus, we may take $t_0 = d/c_0$ ($d$ = detector distance). The real part of the frequency for waves with wave number $K_m$ is of the order of $\nu_m = c_0 K_m$. Thus, to be able to calculate accurately the response to the $\delta$-function source we require that our theory for the dispersion relation be valid up to the frequency $\nu_m$ [see Eq. (51)]. It turns out that this is a problem only at the lowest temperature (0.25 °K) and the smallest propagation distance ($d$ = 0.5 cm). To avoid this difficulty we have, for this temperature only, replaced the $\delta$-function source by a Gaussian $e^{-x^2/a^2}$ with $a$ = 0.025 cm. This corresponds physically to a pulse of duration approximately $2a/c_0$ or 2 $\mu$sec. In Table II we have cal-

TABLE II. Velocities of the front and peak of heat pulses as a function of temperature and propagation distance.

| Temperature (°K) | Detector distance (cm) | Velocity ($10^4$ cm sec$^{-1}$) Isotropic model Front | Isotropic model Peak | Refraction model Front | Refraction model Peak |
|---|---|---|---|---|---|
| 0.25 | 0.5 | 2.31 | 2.25 | 2.33 | 2.31 |
| | 1 | 2.31 | 2.25 | 2.32 | 2.30 |
| | 2 | 2.31 | 2.25 | 2.32 | 2.29 |
| 0.35 | 0.5 | 2.31 | 2.14 | 2.32 | 2.22 |
| | 1 | 2.26 | 2.04 | 2.28 | 2.15 |
| | 2 | 2.20 | 1.92 | 2.23 | 2.04 |
| 0.45 | 0.5 | 2.21 | 1.94 | 2.24 | 2.06 |
| | 1 | 2.12 | 1.82 | 2.16 | 1.93 |
| | 2 | 2.02 | 1.66 | 2.08 | 1.77 |
| 0.6 | 0.5 | 2.07 | 1.70 | 2.10 | 1.82 |
| | 1 | 1.93 | 1.53 | 1.96 | 1.62 |
| | 2 | 1.79 | 1.47 | 1.81 | 1.49 |

culated the velocity of the front of the Gaussian pulses by using for the distance travelled the distance of the detector from the *front* of the pulse at $t=0$.

The principle features of the results are:

(a) The peak of the pulse has a velocity nearly equal to $c_0$ at 0.25 °K (Table II). This velocity decreases with increasing temperature and is approximately equal to $c_0/\sqrt{3}$ at 0.6 °K. At first sight it is tempting to view this variation of velocity as indicating ballistic propagation of individual phonons at low temperatures and collective propagation (i.e., second sound) at high temperatures. It must be remembered, however, that even at 0.25 °K the small-angle mean free path for a typical thermal phonon is still less than $10^{-2}$ cm. Thus, propagation over distances of the order of 1 cm cannot be truly ballistic. The pulses propagate with a velocity close to $c_0$ because the collisions are small angle, typically less than 5° at 0.25 °K. On the basis of our results for the small-angle mean free path, true ballistic propagation is only to be expected below 0.1 °K.

(b) As the propagation distance increases, the pulses broaden and the velocity of the front of the pulse decreases. This occurs because the high-frequency components in the pulse are attenuated more (see Figs. 6 and 8) and because these components have higher velocity (see Figs. 7 and 9).

(c) For the refraction model at 0.25 °K, $\langle \Delta T \rangle$ becomes negative immediately following the arrival of the main signal. A study of the terms in the sum on the right-hand side of Eq. (72) reveals that the main negative contribution to $\langle \Delta T \rangle$ comes from second second-sound waves. We may therefore regard the negative region following the main pulse as a pulse of second second sound. The sign of this pulse is opposite to that of the first second-sound pulse because of the phase difference discussed in Sec. IV A. The negative pulse disappears at higher temperatures because the first second-sound pulse develops a positive tail and the attenuation of second second sound becomes large. For the isotropic model both pulses are positive. The second second-sound pulse then arrives in the tail of the first second-sound pulse. This tail is much larger on the isotropic model than on the refraction model. Analysis of the sum in Eq. (72) shows that the main contribution in the tail is from first second-sound waves of low frequency. The distribution functions associated with these waves vary slowly with $\theta$ [see Figs. 5(a) and 5(b)]. Hence, they are much more strongly coupled to the source in the isotropic model than in the refraction model.

(d) The velocities of both the front and the peak of the pulse are greater for the refraction model than for the isotropic model (Table II). This happens principally because the refraction-model boundary condition couples more strongly to high-$K$ Fourier components, which have a higher velocity.

A large number of studies of pulse propagation in the temperature range below 0.6 °K have been reported.[8-14] As we have mentioned in the Introduction, these experiments all show that the pulse velocity increases as the temperature is lowered, but the various measurements of the pulse velocity are not in quantitative agreement with each other. Some of the reasons for the disagreement between the different experiments are the following:

(i) Different experiments used different propagation distances, and our results show that the pulse velocity depends upon distance.

(ii) Most of the experiments involved the propagation of pulses along tubes filled with helium. Unless the tube diameter is much greater than the propagation distance, there are complicated changes in pulse shape arising from the reflection of the pulse at the walls of the tube. These can give rise to changes in the measured velocity of the peak of the pulse.

(iii) Various ratios of source dimensions to propagation distance were used. One would expect that the velocity of the peak of the pulse should decrease as the size of the source increases.

(iv) The details of the phonon distribution produced by the source are unknown, and are probably different in the various experiments. Our calculations predict considerable variation in the pulse velocity for different initial phonon distributions.

(v) A variety of pulse lengths and pulse shapes were used in the experiments. A longer pulse will be composed of Fourier components with smaller wave numbers and according to our results should travel more slowly.

Because of these uncertainties, it seems hopeless to attempt a quantitative comparison between our calculations and the experiments. An examination of the experimental results reveals nothing that is inconsistent with our calculations, allowing for the uncertainties associated with (i)–(v) above. Experiments under better-defined conditions (i.e., with a large plane source, short pulses, and no wall reflections) are currently being attempted.[35] Even these experiments will still suffer from uncertainties in the initial phonon distribution.

### C. Resonance methods

A standard method for studying second sound above 1 °K is the resonance method.[3,6] This uses a closed tube with a heater at one end. If the frequency is sufficiently high, the two-fluid model

is a good approximation. This enables one to derive simple boundary conditions at the walls and end of the tube. These in turn enable the velocity of second sound to be determined from the frequencies at which resonance occurs. Unfortunately, at temperatures in the range of interest here, the situation is more complicated. A first second-sound wave at normal incidence onto a plane surface will not, in general, be perfectly reflected, even if the surface is a perfect thermal insulator and does not absorb phonons. Other waves (second second sound etc.) will be generated. The part of the first second-sound wave that is reflected will suffer a phase shift, which, in general, will depend upon frequency, temperature, and the details of the surface conditions. Because of these difficulties, the resonance method does not appear promising for studying the dispersion relation of second sound. This conclusion is consistent with the observations of Peshkov,[7] who found that resonance could not be observed below 0.5 °K.

## V. DISCUSSION

Let us consider first why there are extra waves in addition to ordinary second sound. To understand this we note that ordinary second sound exists as a propagating wave because energy and momentum are conserved in collisions between excitations in superfluid helium. In crystalline solids momentum is not conserved (except in special circumstances) and a temperature wave with a real wave number has a purely imaginary frequency. This suggests that the presence of extra waves at low temperatures is connected with the existence of additional conserved quantities. Of course, there are no additional quantities that are exactly conserved. However, if there exists a quantity that relaxes very little during one period of the sound wave, we may regard this as "sufficiently conserved". In the present case quantities of this type are the amplitudes $A_{1l}$ of the $n=1$ states with $l \geq 2$. Let us call the coefficients $A_{12}, A_{13}$, etc., the $D$-ness, $F$-ness, etc. respectively. In this notation the total energy of the phonons is proportional to the $S$-ness of the distribution and this is a conserved quantity, as is the $P$-ness. The $D$-ness relaxes in a time $\lambda_{12}^{-1}$. Thus, if

$$\Omega \gg \lambda_{12},$$

the $D$-ness may be regarded as a conserved quantity in nearly the same right as energy and momentum. As $\Omega$ increases, extra quantities become conserved and new propagating waves appear. We note that the two-fluid theory of helium describes the state of the phonon system by just two variables, the energy and momentum densities. These variables are chosen because they are the only rigorously conserved quantities and thus at low frequencies they will dominate the hydrodynamic behavior. We may regard the present theory as a generalized hydrodynamics in which the state of the system is described not only by rigorously conserved quantities but also by the most slowly relaxing nonconserved quantities.

It is interesting to try to understand the frequency and temperature dependence of the attenuation and velocity using the conventional theory of relaxation processes. For a system with a set of relaxation times $\{\tau_i\}$ the attenuation and velocity of a wave with frequency $\Omega$ are

$$\alpha = \sum_i f_i \frac{\Omega^2 \tau_i}{1+\Omega^2 \tau_i^2}, \tag{73}$$

$$c = c_{1f} + \sum_i g_i \frac{\Omega^2 \tau_i^2}{1+\Omega^2 \tau_i^2}. \tag{74}$$

$c_{1f}$ is the low-frequency limiting value of the velocity, and $f_i$ and $g_i$ measure the strengths of the different relaxation processes. $f_i$ and $g_i$ are connected by the Kramers-Kronig relation, and if the relaxation is weak they are constants independent of $\Omega$. We try to use these equations by identifying $\tau_l$ with the lifetime of the $l$th $n=1$ state. Thus we set

$$\tau_l = \lambda_{1l}^{-1}. \tag{75}$$

The sums in (73) and (74) now go from 2 to $\infty$. The attenuation and velocity of first second sound may be understood qualitatively in this way. At a given temperature the velocity increases monotonically with increasing frequency (see Fig. 7) as predicted by (74). Moreover, Eq. (74) predicts that the velocity should start to deviate from its low-frequency limit when $\Omega$ becomes comparable to the inverse of the longest relaxation time. In the present case this relaxation time is $\tau_2 (\equiv \lambda_{12}^{-1})$. The numerical results for the velocity dispersion do in fact show just this behavior, i.e., at each temperature the velocity of first second sound begins to increase from its low-frequency limiting value when $\Omega\tau_2$ becomes of the order of unity. Note that the velocity results do not show a sequence of clearly resolved relaxations associated with each of the set of times $\{\tau_l\}$. This is simply because the different relaxation times are sufficiently closely spaced that the relaxation connected with the $l$th time has not been completed before the $(l+1)$th relaxation begins.

When $\Omega\tau_l$ is much less than 1 for all values of $l$ the attenuation is

$$\alpha \approx \sum_{l=2}^{\infty} f_l \Omega^2 \tau_l . \tag{76}$$

Since the $\{\tau_l\}$ increase as the temperature goes down, this formula should hold at low frequencies and high temperatures. At 0.5 °K $\tau_2$ is 6 $\mu$sec and thus $\Omega\tau_2 \sim 1$ at a frequency of about 25 kHz. Hence for frequencies less than this the attenuation should be proportional to the $\{\tau_l\}$ and should increase as the temperature is lowered. This is in agreement with the numerical results (see Fig. 6). At high frequencies and low temperatures, on the other hand, the position will be more complicated since $\Omega\tau_l$ will be greater than 1 for small values of $l$, but less than 1 for large $l$. Thus we may write

$$\alpha \approx \sum_{l=2}^{l_c} \frac{f_l}{\tau_l} + \sum_{l_c+1}^{\infty} f_l \Omega^2 \tau_l , \tag{77}$$

where $l_c$ is the largest value of $l$ for which $\Omega\tau_l > 1$. The two terms in (77) have opposing temperature dependences and thus we are unable to use the relaxation theory to predict the temperature dependence of the attenuation. The numerical results (Fig. 6) give the attenuation decreasing as $T$ decreases in the low-temperature regime. This implies that it is the first term that dominates in (77). Physically, this means that the relaxation strength must be greatest for small $l$.

An observation of second second sound would be very interesting. The most promising experimental technique would appear to be the sine-wave method discussed in Sec. IV A. In principle, this technique can provide complete information about the dispersion relation and attenuation of the waves. A measurement of the relative phase of first and second second sound would give useful information about how phonons radiate into helium from a heated surface. If accurate measurements can be made of the attenuation and velocity of the waves, it might be possible to work backwards to obtain information about the details of the phonon dispersion relation. The theoretical predictions for the attenuation and velocity are quite sensitive to small changes in the assumed form of the phonon-dispersion relation (see Figs. 6–9). A similar experimental study under pressure would also be of interest. The parameter $\gamma$ entering into the dispersion relation is believed to change sign before the freezing pressure is reached.[22] When this happens, the three-phonon scattering process that we have considered as the dominant scattering mechanism becomes unallowed. The most important scattering processes will then be either the three-phonon process in second order, or a four-phonon process. This change should be reflected in a considerable modification of the dispersion relations for second-sound waves. Evidence that the propagation characteristics of heat pulses undergo considerable change at high pressure has been reported recently by Dynes *et al.*[14]

I should like to thank D. V. Osborne, G. Niklasson, and A. Sjölander for a number of valuable discussions, and Professor R. W. Guernsey and Professor K. Lusczynski for correspondence about their experiments.

---

*Work supported in part by the National Science Foundation.

†Science Research Council Senior Visiting Fellow for the year 1972–73.

‡Permanent address.

[1]L. Tisza, Compt. Rend. 207, 1035 (1938); Compt. Rend. 207, 1186 (1938).

[2]L. D. Landau, J. Phys. (USSR) 5, 71 (1941).

[3]V. P. Peshkov, J. Phys. (USSR) 8, 381 (1944); J. Phys. (USSR) 10, 389 (1946); and in *Proceedings of the Conference on Low Temperature Physics* (Physical Society, London, 1947), p. 19.

[4]For a discussion of second sound and kinetic processes in helium, see J. Wilks, *The Properties of Liquid and Solid Helium* (Oxford U. P., London, 1967).

[5]W. M. Whitney and C. E. Chase, Phys. Rev. 158, 200 (1967).

[6]V. P. Peshkov, Zh. Eksp. Teor. Fiz. 23, 686 (1952).

[7]V. P. Peshkov, Zh. Eksp. Teor. Fiz. 38, 799 (1960) [Sov. Phys.—JETP 11, 580 (1960)].

[8]K. R. Atkins and D. V. Osborne, Philos. Mag. 41, 1078 (1950).

[9]V. Mayper and M. A. Herlin, Phys. Rev. 89, 523 (1953).

[10]D. de Klerk, R. P. Hudson, and J. R. Pellam, Phys. Rev. 89, 326 (1953); Phys. Rev. 93, 28 (1954).

[11]H. C. Kramers, F. A. W. van den Burg, and C. J. Gorter, Phys. Rev. 90, 1117 (1953).

[12]H. C. Kramers, T. van Peski-Tinbergen, J. Wiebes, F. A. W. van den Burg, and C. J. Gorter, Physics 20, 743 (1954).

[13]R. W. Guernsey and K. Luszczynski, Phys. Rev. A 3, 1052 (1971).

[14]R. C. Dynes, V. Narayanamurti, and K. Andres, Phys. Rev. Lett. 30, 1129 (1973).

[15]D. V. Osborne, Philos. Mag. 1, 301 (1956).

[16]This assumption is valid in the present context provided that $\rho_n$ is much less than $\rho_s$.

[17]G. Leibfried, in *Handbuch der Physik*, edited by S. Flügge (Springer, Berlin, 1955), Vol. 7.

[18]H. J. Maris, Phys. Rev. Lett. 30, 312 (1973).

[19]H. J. Maris, Phys. Rev. A 7, 2074 (1973).

[20]H. J. Maris, Phys. Rev. A 8, 1980 (1973).

[21]A. D. B. Woods and R. A. Cowley, Phys. Rev. Lett. 24, 646 (1970); Can. J. Phys. 49, 177 (1971).

[22]N. E. Phillips, C. G. Waterfield, and J. K. Hoffer, Phys. Rev. Lett. 25, 1260 (1970).
[23]R. W. Whitworth, Proc. Roy. Soc. Lond. A 246, 390 (1958).
[24]B. M. Abraham, Y. Eckstein, J. B. Ketterson, M. Kuchnir, and P. R. Roach, Phys. Rev. A 1, 250 (1970); Phys. Rev. A 2, 550 (1970).
[25]For dispersion curves C and D phonons of energy up to about 8 °K are able to decay by a three-phonon process.
[26]J. Jäckle, Phys. Kondens. Mater. 11, 139 (1970).
[27]F. M. Claro and G. H. Wannier [J. Math. Phys. 12, 92 (1970)] have also studied the $S$-state eigenfunctions for a system of phonons undergoing three-particle collisions. For a special form of the matrix-element they are able to find these eigenfunctions analytically. Their result contains a singularity of the form (32) located at a value of $\epsilon_c$ given by (33).
[28]This is true if we ignore the upper energy limit of the three-phonon process.
[29]For a weakly interacting Bose gas, transverse waves ($\mu = 1$) have been considered by S.-K. Ma, Phys. Rev. A 5, 2632 (1972).
[30]This equation has also been derived for a weakly-interacting Bose gas by S.-K. Ma [J. Math. Phys. 12, 2157 (1971)] using a completely microscopic approach. Note that there is an error in Ma's result for the eigenvalues of the $n = 1$ states [his Eq. (5.43)]. A corrected result is Eq. (A2) of Ref. 20.
[31]L. D. Landau and I. M. Khalatnikov, Zh. Eksp. Teor. Fiz. 19, 637 (1949). Several approximations are made to derive this result. In addition, there are uncertainties in some of the parameters involved. See, I. M. Khalatnikov, *Introduction to the Theory of Superfluidity* (Benjamin, New York, 1965), p. 47.
[32]Direct evidence that phonons are refracted when passing from a solid into helium has been obtained by R. A. Sherlock, A. F. G. Wyatt, N. G. Mills, and N. A. Lockerbie, Phys. Rev. Lett. 29, 1299 (1972).
[33]We could also calculate the evolution of a pulse by direct numerical integration of Eq. (12) using the initial condition (69).
[34]The peculiar units of temperature appear because of the initial condition (69).
[35]D. V. Osborne and J. Cowey (private communication), and C. Elbaum and W. Junker (private communication).